Room-Temperature Laser Emission of ZnO Nanowires Explained by Many-Body Theory

Marijn A. M. Versteegh,[1] Daniël Vanmaekelbergh,[1] and Jaap I. Dijkhuis[1,*]

[1]*Debye Institute for Nanomaterials Science, Utrecht University, Princetonplein 1, 3584 CC Utrecht, The Netherlands*

(Received 16 January 2012; published 12 April 2012)

Are excitons involved in lasing in ZnO nanowires or not? Our recently developed and experimentally tested quantum many-body theory sheds new light on this question. We measured the laser thresholds and Fabry-Pérot laser modes for three radically different excitation schemes. The thresholds, photon energies, and mode spacings can all be explained by our theory, without invoking enhanced light-matter interaction, as is needed in an earlier excitonic model. Our conclusion is that lasing in ZnO nanowires at room temperature is not of excitonic nature, as is often thought, but instead is electron-hole plasma lasing.

DOI: 10.1103/PhysRevLett.108.157402 PACS numbers: 78.67.Uh, 78.20.Bh, 78.45.+h

Theories that predict the electronic structure of semiconductor crystals on the single-particle level have been instrumental in the understanding of the electrical and optical properties of most semiconductor systems, including semiconductor nanostructures. However, for semiconductors with high doping or under conditions of strong excitation, the effects of band-filling and carrier-carrier interactions become prominent and a description on the single-particle level often fails. In those cases, the solid-state band theory has to be complemented with many-body interactions for a better understanding [1,2].

A prime example is room-temperature lasing of ZnO nanowires. Here, it has often been stated that the lasing is due to scattering processes that involve excitons, at least, if the excitation intensity is not too far above the laser threshold [3–14]. Excitons are hydrogen-atom-like electron-hole pairs, bound by the Coulomb force. The idea is that excitons, which are known to play an essential role in lasing in ZnO at cryogenic temperatures [15,16], survive at room temperature, because their binding energy is 60 meV, considerably larger than $k_B T$ (25 meV). For increasing electron-hole pair density, screening reduces the Coulomb attraction, and therefore also the fraction of excitons. Above the so-called ''Mott density,'' excitons cease to exist, and the charge carriers form an electron-hole plasma. Indeed, in case excitation is far above laser threshold, lasing is claimed to make a transition from excitonic lasing to electron-hole plasma lasing [4,6,7,9,11,14]. On the other hand, Klingshirn *et al.* [17] argue that excitons are probably not involved in most cases of room-temperature lasing in ZnO, even not just above threshold. Many-body theory should solve this long-standing problem.

Recently, we developed a quantum many-body theory to describe the optical properties of a high-density interacting electron-hole gas in ZnO [18]. It was successful in explaining the light reflection from macroscopic crystals of ZnO at room temperature at various excitation intensities [18], as well as stimulated emission from preformed electron-hole Cooper pairs at cryogenic temperatures [19]. Using our theory, we calculated that the Mott density in ZnO equals 1.5×10^{24} m^{-3} at $T = 300$ K, and we argued that this is a more accurate result than was obtained by others. This value was confirmed in a pump-probe reflectivity experiment by the gradual disappearance of the exciton resonance when passing this electron-hole density [18]. In this Letter, we use the same theory to determine the laser mechanism in ZnO nanowires at room temperature. We compare the theory with experimental results, where we excited ZnO nanowires in three radically different ways. Our results consistently show that room-temperature lasing in ZnO nanowires occurs in the electron-hole plasma regime. Moreover, many-body theory can excellently explain the observed laser threshold, the photon energy of the laser emission, and the spectral spacings between the laser peaks.

The usual method of exciting a ZnO nanowire is by a laser pulse. The electron-hole density in the wire can be calculated from the time-dependent pump intensity $I(t)$ inside the nanowire. For a Gaussian pulse we have $I(t) = Fe^{-t^2/(2d^2)}/(\sqrt{2\pi}d)$, where F is the fluence (in J/m^2 per pulse) inside the nanowire, just behind the surface, and d is $1/\sqrt{8\ln 2}$ times the pulse duration (full width at half maximum). We distinguish three different pump schemes: (1) Direct excitation with nanosecond pulses at photon energies higher than the band gap. Here, the electron-hole density reached depends on the carrier decay time. For a nanowire oriented perpendicular to the propagation direction of the excitation light, the time-dependent average electron-hole density in the nanowire follows from the rate equation

$$\frac{dn(t)}{dt} = \frac{I(t)}{\hbar\omega D} - \frac{n(t)}{\tau}, \tag{1}$$

where $\hbar\omega$ is the photon energy and D is the diameter of the wire. We assume here that the wire diameter exceeds the penetration depth of the pump pulse (50 nm), so that

virtually all photons entering the wire are absorbed. (2) Excitation with femtosecond or picosecond pulses at photon energies higher than the band gap. This excitation method has the advantage that carrier decay during the pump pulse can be ignored, so that the electron-hole density can be determined more accurately. For the same perpendicular nanowire orientation, the average density in the wire after the pump pulse is simply given by

$$n = F/(\hbar\omega D). \quad (2)$$

(3) Excitation with high-intensity femtosecond pulses at photon energies below the band gap via two- or three-photon absorption. In this method, the excitation profile is homogeneous, due to a long penetration depth. In case of three-photon absorption, the electron-hole density is to be calculated from

$$\frac{dn(t)}{dt} = \frac{\alpha_3[I(t)]I(t)^3}{3\hbar\omega}, \quad (3)$$

where $\alpha_3[I(t)]$ is the intensity-dependent three-photon absorption coefficient.

Using these equations, we computed the electron-hole pair densities at the laser threshold from the pump fluences given in the literature. On the basis of reported carrier and exciton lifetimes in ZnO below the laser threshold [20–26], and our pump-probe reflectivity results [18], we took $\tau =$ 400 ps for the carrier decay time, and for $\alpha_3[I(t)]$ we took the values as reported in Ref. [18]. We find that the vast majority of reported laser thresholds [5–9,12,13,27–32] actually lie above the Mott density, between 1.5×10^{24} m^{-3} and 1.5×10^{26} m^{-3}. Only one group reported a lower threshold [3,4,24]. This indicates that, at least for the majority of cases, room-temperature lasing in ZnO nanowires does not involve excitons. Parameters affecting the laser threshold are the nanowire dimensions [13,33], the quality of the nanowire, which is strongly dependent on the growth conditions [34], and the substrate supporting the wire [35].

The first aim of our experiment is to determine the electron-hole density at the laser threshold as reliably as possible, by using the three different pump schemes as described above. We excited ZnO nanowires by 5 ns 355 nm pulses from a 50 Hz Nd:YAG laser, and by 120 fs 267 nm and 120 fs 800 nm pulses from an amplified 1 kHz Ti:sapphire laser. For one nanowire we used 10 ns 349 nm pulses from a 1.6 kHz Nd:YLF laser.

We performed extensive measurements on ten nanowires [36], with lengths varying between 4.8 μm and 23.5 μm. The laser thresholds densities are summarized in Table I. For the wires *B*, *G*, and *H*, where different excitation methods could be applied, we obtained roughly the same threshold densities, supporting the consistency of our determination of the electron-hole density inside the wires. Clearly, all determined threshold densities are far above the Mott density (1.5×10^{24} m^{-3}), from which we conclude that the lasing we observe, occurs in the electron-hole plasma regime.

TABLE I. Electron-hole densities at the laser threshold inside ten ZnO nanowires. Laser action was produced by four different excitation methods. The density was calculated using Eqs. (1)–(3). For 800 nm excitation also the angle of the polarization with respect to the nanowire axis is given.

Nanowire	Length (μm)	Excitation pulse	Threshold density (10^{25} m^{-3})
A	4.8	10 ns 349 nm	5.1
B	4.8	5 ns 355 nm	13
		120 fs 267 nm	16
		120 fs 800 nm +3°	28
C	7.6	120 fs 800 nm −83°	48
D	8.9	120 fs 800 nm −77°	98
E	9.9	120 fs 800 nm −14°	9.3
F	15.0	120 fs 800 nm −72°	8.5
G	17.1	5 ns 355 nm	23
		120 fs 267 nm	16
		120 fs 800 nm 0°	21
H	18.1	120 fs 267 nm	41
		120 fs 800 nm −22°	56
I	21.0	120 fs 800 nm 0°	5.2
J	23.5	120 fs 267 nm	6.7

As an example, Fig. 1 shows images of nanowire *G* and emission spectra just above the laser threshold. On this wire, we used 5 ns 355 nm, 120 fs 267 nm, and 120 fs 800 nm excitation. Calculation of the laser threshold density from the pump fluence, using Eqs. (1)–(3), yields for all three methods roughly the same value of 2×10^{26} m^{-3}. The peak at 3.10 eV originates from second-harmonic generation of 800 nm light [37]. The relative emission intensity of 120 fs excitation compared to 5 ns excitation agrees with a carrier decay time of about 400 ps.

The observed electron-hole densities and laser emission photon energies at the laser threshold can be accounted for by our many-body theory [18]. Optical absorption and

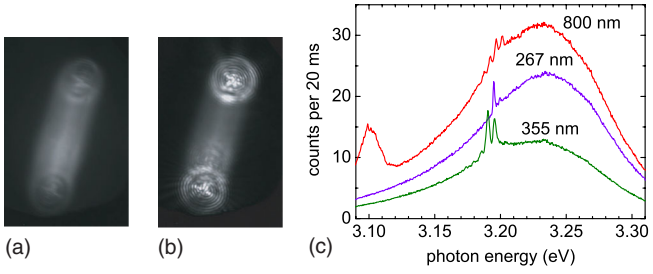

FIG. 1 (color online). Laser action in ZnO nanowire *G*. (a) UV image just above laser threshold. Excitation: 120 fs 267 nm pulses at 27.5 J/m^2. (b) UV image for intense laser action. Excitation: 120 fs 267 nm pulses at 36.2 J/m^2. (c) Emission spectra just above laser threshold pumped by 50 Hz 5 ns 355 nm, 1 kHz 120 fs 267 nm, and 1 kHz 120 fs 800 nm pulses. Fluences *F* were 405 J/m^2, 27.5 J/m^2, and 1158 J/m^2, respectively.

refractive index spectra of highly excited ZnO are calculated by deriving and subsequently solving the statically screened Bethe-Salpeter ladder equation for an electron-hole gas interacting with an electromagnetic field. Calculations were performed for polarization perpendicular to the c axis of the ZnO crystal, which is the polarization of light propagating through a ZnO nanowire. Negative absorption, i.e., gain, appears at $n = 2 \times 10^{25}$ m^{-3} [Fig. 2(a)]. This electron-hole density is in good agreement with the laser threshold densities specified in Table I, given the fact that waveguide losses and transmission losses at the wire end facets increase the laser threshold to a somewhat higher level. For nanowires with defects, the laser threshold is further raised. All gain in the theory results from stimulated emission by an inverted electron-hole plasma. In some cases in the literature the threshold density is between 1.5×10^{24} m^{-3} and 2×10^{25} m^{-3}. Here, gain is probably due to an electron-hole plasma in which carrier-carrier and carrier-phonon collisions contribute to the stimulated emission, as discussed in Ref. [17]. These effects are not included in our theory. We note that the actual gain is lower than the theoretical values given in Fig. 2(a), as a result of damping and losses, depending on the quality of the wire under investigation. Recently, Richters *et al.* [38] measured the modal gain spectrum of a single ZnO nanowire and found a maximum of 0.4 μm^{-1} at 3.24 eV.

The laser emission photon energy of a ZnO nanowire at room temperature is typically about 3.2 eV, as can be seen, for example, in Fig. 1. According to the theoretical absorption spectra [Fig. 2(a)], the theoretical emission photon energy at the laser threshold equals 3.23 eV, close to the experimental values. For stronger excitation, more laser peaks show up in our experiment, both on the low- and high-energy sides. In agreement with this, the theory shows a broadening of the spectral range where gain occurs. When comparing experimental data with theory, one must realize that the precision of the theoretical calculation

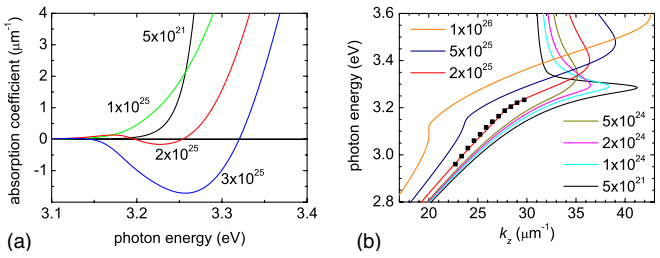

FIG. 2 (color online). Results of our many-body theory for ZnO at $T = 300$ K for polarization $\mathbf{E} \perp c$. Electron-hole densities are indicated in m^{-3}. (a) Absorption spectra at four electron-hole pair densities. Gain starts at 2×10^{25} m^{-3}. (b) Dispersion relations ($m_x = m_y = 1$) for light inside a ZnO nanowire with dimensions $L_x = L_y = 200$ nm for several densities. Squares indicate measured Fabry-Pérot modes, as reported in Ref. [10], Fig. 3(c).

of the band-gap renormalization is limited, and that the variation of the electron-hole density in time, and possibly also in space, affects the lasing behavior.

The observed positions of the Fabry-Pérot laser peaks can be explained from many-body theory by computing the dispersion relations of light inside a ZnO nanowire. A ZnO nanowire acts as a small cavity for light. For a rectangular wire with dimensions L_x, L_y, and L_z, the wave vector k obeys $k^2 = k_x^2 + k_y^2 + k_z^2$, with $k_i = m_i \pi / L_i$, where m_i is a positive integer. For a wire with a diameter of about 200 nm, the laser mode is the lowest transverse electric mode, the TE_{01} mode [10,13,33], in this model the mode with quantum numbers $m_x = m_y = 1$. This confinement of light between the end-facets of the wire leads to lasing at several Fabry-Pérot peaks. The spacing between the peaks is determined by the length of the wire and the slope of the dispersion relation. The dispersion relation between the photon energy and k_z, the wave vector in the direction of the wire, is given by

$$\hbar\omega = \frac{\hbar c}{n'(\omega, n)} \sqrt{(m_x \pi / L_x)^2 + (m_y \pi / L_y)^2 + k_z^2}, \quad (4)$$

where $n'(\omega, n)$ is the frequency- and density-dependent real part of the refractive index of ZnO, which is computed in the many-body theory. The laser peaks of a nanowire correspond to subsequent values of m_z. Dispersion relations for a 200 nm thick nanowire are shown in Fig. 2(b). At low electron-hole densities we recognize a damped exciton-polariton dispersion relation. We stress that this result is obtained from first principles, not by modeling $n'(\omega, n)$ by a Lorentz model.

One argument for excitonic lasing, used in Ref. [10], is that the spacing between the observed laser peaks is consistent with the exciton-polariton dispersion relation. As an example, a fit was shown in Ref. [10] for a lasing ZnO nanowire of about 170 nm in diameter and 5 μm in length. The agreement is, indeed, very good. However, damping was neglected, and a 5 times stronger light-matter coupling than in bulk ZnO was required to fit the data with the Lorentz-type exciton-polariton equation. The experimental results of Ref. [10], however, can be equally accurately explained by our many-body theory, *without* the introduction of any additional features. Comparing the measured laser peaks with our theoretical dispersion relations for a diameter of 200 nm, close to that determined from scanning electron microscopy, we find that there is a very good fit at $n = 2 \times 10^{25}$ m^{-3} [Fig. 2(b)], which is clearly above the Mott density. Damping is taken into account in our theory. More importantly, the light-matter coupling inside the nanowire is taken equal to the bulk value and is a fixed parameter in our theory.

Unfortunately, we have no direct access to the absolute values of k_z from the Fabry-Pérot modes. Known are, however, the photon energies of the laser peaks, and, via the length of the wire, the difference in k_z between

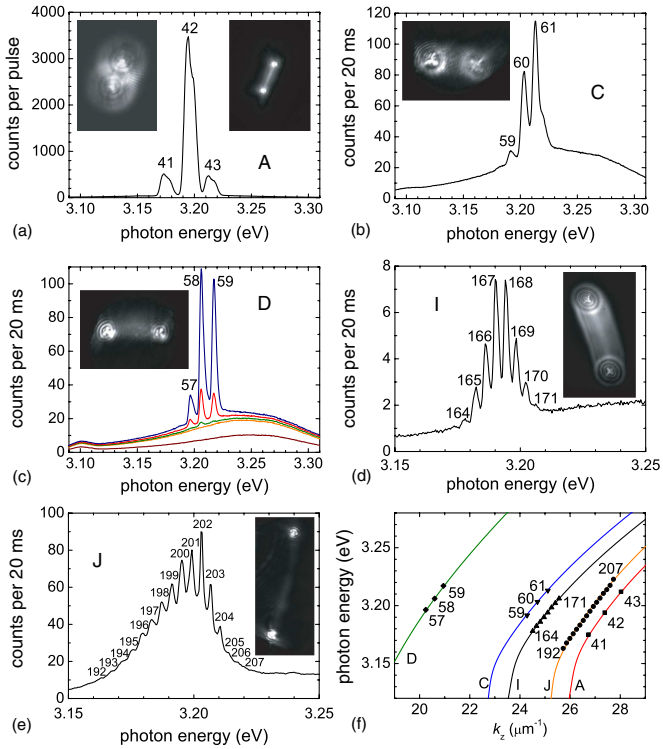

FIG. 3 (color online). Spacings between measured Fabry-Pérot laser modes explained by many-body theory. (a) Emission spectrum of nanowire A. Excitation: 10 ns 349 nm pulses at $F = 355$ J/m^2. Fabry-Pérot mode numbers m_z are indicated. Left inset shows coherence fringes between light emerging from the two ends of the wire. Right inset has wire in focus. (b) Nanowire C. Excitation: 120 fs 800 nm pulses at 1585 J/m^2. (c) Nanowire D. Excitation: 120 fs 800 nm pulses at 1619, 1904, 1940, 1974, and 2050 J/m^2. (d) Nanowire I. Excitation: 120 fs 800 nm pulses at 729 J/m^2. (e) Nanowire J. Excitation: 120 fs 267 nm pulses at 25 J/m^2. (f) Fabry-Pérot modes of A fitted to the theoretical dispersion relation ($m_x = m_y = 2$) for a 460 nm thick nanowire at $n = 5 \times 10^{25}$ m^{-3}. Fabry-Pérot modes of C, D, and I fitted to the dispersion relation ($m_x = m_y = 1$) for a 200 nm thick nanowire at densities $n = 6 \times 10^{25}$ m^{-3}, 1.3×10^{26} m^{-3}, and 5×10^{25} m^{-3}, respectively. Fabry-Pérot modes of J fitted to the dispersion relation ($m_x = m_y = 1$) for a 230 nm thick nanowire at $n = 6 \times 10^{25}$ m^{-3}.

subsequent Fabry-Pérot modes. Fitting the experimental data to theory is by moving the squares in Fig. 2(b) in the horizontal direction until the best match with a dispersion curve is found. Note that not only the slope of the dispersion curve at $n = 2 \times 10^{25}$ m^{-3}, but also the bending around 3.2 eV, excellently fits the experimental points. In contrast, the exciton-polariton dispersion relations at densities below the Mott density in Fig. 2(b) cannot fit the experimental data at all, without the introduction of extra parameters.

In our own experiments, we find a regular spacing between the laser modes in the spectrum for most nanowires. The experimental results for several of these nanowires are presented in Fig. 3. In Fig. 3(f), the spectral

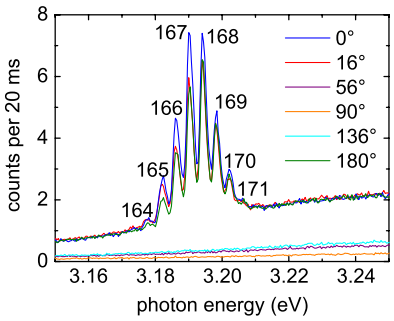

FIG. 4 (color online). Emission spectra of nanowire I for different angles between the polarization of the 800 nm pump pulse and the nanowire axis.

positions of the measured Fabry-Pérot laser modes are fitted to the theoretical dispersion relations. For nanowires A, I, and J there is a good fit with the dispersion relations that were calculated at the threshold densities (Table I). For nanowires C and D a good fit is obtained below the experimental threshold densities, but still far above the Mott density. This deviation is probably due to the large angle between the nanowire axis and the polarization of the 800 nm excitation light: 83° for nanowire C and 77° for nanowire D. We observed for several wires that the emission is stronger for 800 nm excitation polarization parallel to the wire, than for polarization perpendicular to the wire. As an example, Fig. 4 shows results for nanowire I. A similar polarization dependency for the case of two-photon absorption was observed before [39]. An explanation for this phenomenon can be found in the work of Wang *et al.* [40], who showed that for excitation fields polarized perpendicular to an InP nanowire, the electric field inside the wire is attenuated, while it is not reduced for polarizations parallel to the wire. Such an attenuation would reduce the three-photon absorption in wires C and D. The actual threshold density of these two wires is therefore probably lower than the values stated in Table I.

Fitting the measured laser modes to theory yields the mode numbers m_x, m_y and the absolute values of k_z and thereby the mode numbers m_z of the measured laser peaks, as indicated in Figs. 3 and 4. Only for the 460 nm thick nanowire A we find $m_x = m_y = 2$. We further observe [Fig. 3(a)] that each of the three peaks actually consists of two laser modes, from which it can be concluded that lasing in nanowire A is probably also mediated by laser modes with other quantum numbers.

In conclusion, lasing in ZnO nanowires at room temperature is electron-hole plasma lasing. Only when special measures are taken to lower the laser threshold, such as mirrors at the ends of the wire, excitonic lasing might become possible [41]. Resonant excitation of excitons, perhaps via two-photon absorption, might be another possibility. Our many-body theory, based on first principles, predicts laser thresholds and laser spectra in excellent agreement with experiments. Theoretical dispersion

relations account for the measured spacing between the Fabry-Pérot laser modes, without invoking increased light-matter coupling, as is needed for an exciton-polariton model.

We thank D. H. van Dorp for growing the ZnO nanowires, C. R. de Kok and P. Jurrius for technical support, and R. Khedoe, D. H. van Dorp, and A. J. van Lange for their help with the measurement with the Nd:YLF laser.

*j.i.dijkhuis@uu.nl

[1] H. Haug and S. W. Koch, *Quantum Theory of the Optical and Electronic Properties of Semiconductors* (World Scientific, Singapore, 2004), 4th ed..
[2] A. Schleife, C. Rödl, F. Fuchs, K. Hannewald, and F. Bechstedt, Phys. Rev. Lett. **107**, 236405 (2011).
[3] M. H. Huang, S. Mao, H. Feick, H. Yan, Y. Wu, H. Kind, E. Weber, R. Russo, and P. Yang, Science **292**, 1897 (2001).
[4] J. C. Johnson, H. Yan, P. Yang, and R. J. Saykally, J. Phys. Chem. B **107**, 8816 (2003).
[5] H. C. Hsu, C. Y. Wu, and W. F. Hsieh, J. Appl. Phys. **97**, 064315 (2005).
[6] W. M. Kwok, A. B. Djurišić, Y. H. Leung, W. K. Chan, and D. L. Phillips, Appl. Phys. Lett. **87**, 093108 (2005).
[7] W. M. Kwok, A. B. Djurišić, Y. H. Leung, W. K. Chan, and D. L. Phillips, H. Y. Chen, C. L. Wu, S. Gwo, and M. H. Xie, Chem. Phys. Lett. **412**, 141 (2005).
[8] C. F. Zhang, Z. W. Dong, G. J. You, S. X. Qian, and H. Deng, Opt. Lett. **31**, 3345 (2006).
[9] J. K. Song, U. Willer, J. M. Szarko, S. R. Leone, S. Li, and Y. Zhao, J. Phys. Chem. C **112**, 1679 (2008).
[10] H. Y. Li, S. Rühle, R. Khedoe, A. F. Koenderink, and D. Vanmaekelbergh, Nano Lett. **9**, 3515 (2009).
[11] S. Mitsubori, I. Katayama, S. H. Lee, T. Yao, and J. Takeda, J. Phys. Condens. Matter **21**, 064211 (2009).
[12] C. Torres-Torres, M. Trejo-Valdez, H. Sobral, P. Santiago-Jacinto, and J. A. Reyes-Esqueda, J. Phys. Chem. C **113**, 13515 (2009).
[13] M. A. Zimmler, F. Capasso, S. Müller, and C. Ronning, Semicond. Sci. Technol. **25**, 024001 (2010).
[14] J. Dai, C. X. Xu, P. Wu, J. Y. Guo, Z. N. Li, and Z. L. Shi, Appl. Phys. Lett. **97**, 011101 (2010).
[15] J. R. Packard, D. A. Campbell, and W. C. Tait, J. Appl. Phys. **38**, 5255 (1967).
[16] J. M. Hvam, Solid State Commun. **12**, 95 (1973).
[17] C. Klingshirn, R. Hauschild, J. Fallert, and H. Kalt, Phys. Rev. B **75**, 115203 (2007).
[18] M. A. M. Versteegh, T. Kuis, H. T. C. Stoof, and J. I. Dijkhuis, Phys. Rev. B **84**, 035207 (2011).
[19] M. A. M. Versteegh, A. J. van Lange, H. T. C. Stoof, and J. I. Dijkhuis, arXiv:1111.4336.
[20] D. C. Reynolds, D. C. Look, B. Jogai, J. E. Hoelscher, R. E. Sherriff, M. T. Harris, and M. J. Callahan, J. Appl. Phys. **88**, 2152 (2000).
[21] T. Koida, S. F. Chichibu, A. Uedono, A. Tsukazaki, M. Kawasaki, T. Sota, Y. Segawa, and H. Koinuma, Appl. Phys. Lett. **82**, 532 (2003).
[22] B. Guo, Z. Ye, and K. S. Wong, J. Cryst. Growth **253**, 252 (2003).
[23] C. Bauer, G. Boschloo, E. Mukhtar, and A. Hagfeldt, Chem. Phys. Lett. **387**, 176 (2004).
[24] J. C. Johnson, K. P. Knutsen, H. Yan, M. Law, Y. Zhang, P. Yang, and R. J. Saykally, Nano Lett. **4**, 197 (2004).
[25] J. Wilkinson, K. B. Ucer, and R. T. Williams, Radiation Measurements **38**, 501 (2004).
[26] A. Teke, Ü. Özgür, S. Doğan, X. Gu, H. Morkoç, B. Nemeth, J. Nause, and H. O. Everitt, Phys. Rev. B **70**, 195207 (2004).
[27] X. Han, G. Wang, Q. Wang, L. Cao, R. Liu, B. Zou, and J. G. Hou, Appl. Phys. Lett. **86**, 223106 (2005).
[28] Y. Zhang, R. E. Russo, and S. S. Mao, Appl. Phys. Lett. **87**, 043106 (2005).
[29] J. K. Song, J. M. Szarko, S. R. Leone, S. Li, and Y. Zhao, J. Phys. Chem. B **109**, 15749 (2005).
[30] L. K. van Vugt, S. Rühle, and D. Vanmaekelbergh, Nano Lett. **6**, 2707 (2006).
[31] V. V. Zalamai, V. V. Ursaki, C. Klingshirn, H. Kalt, G. A. Emelchenko, and A. N. Redkin, Appl. Phys. B **97**, 817 (2009).
[32] J. Fallert, R. J. B. Dietz, H. Zhou, J. Sartor, C. Klingshirn, and H. Kalt, Phys. Status Solidi C **6**, 449 (2009).
[33] A. V. Maslov and C. Z. Ning, Appl. Phys. Lett. **83**, 1237 (2003).
[34] D. J. Gargas, H. Gao, H. Wang, and P. Yang, Nano Lett. **11**, 3792 (2011).
[35] S. Wang, Z. Hu, H. Yu, W. Fang, M. Qiu, and L. Tong, Opt. Express **17**, 10881 (2009).
[36] The wires were epitaxially grown on a sapphire substrate, using the carbothermal reduction method with gold particles as catalysts [37]. Temperatures in the range of 890°C to 920°C were used, to obtain maximum quantum efficiency [34]. Subsequently, the wires were mechanically broken off and dispersed onto a sapphire substrate. The *c* axis of the ZnO crystal was directed along the wires. The UV emission from the excited nanowires was collected by an objective and imaged on a CCD camera. Simultaneously, the emission spectrum was measured by a spectrometer, coupled to a liquid-nitrogen-cooled CCD camera. An autocorrelator was used to regularly check the pulse length of the Ti:sapphire laser.
[37] R. Prasanth, L. K. van Vugt, D. A. M. Vanmaekelbergh, and H. C. Gerritsen, Appl. Phys. Lett. **88**, 181501 (2006).
[38] J. P. Richters, J. Kalden, M. Gnauck, C. Ronning, C. P. Dietrich, H. von Wenckstern, M. Grundmann, J. Gutowski, and T. Voss, Semicond. Sci. Technol. **27**, 015005 (2012).
[39] L. K. van Vugt, Ph.D. thesis, Utrecht University, 2007.
[40] J. Wang, M. S. Gudiksen, X. Duan, Y. Cui, and C. M. Lieber, Science **293**, 1455 (2001).
[41] A. N. Gruzintsev, G. A. Emelchenko, A. N. Redkin, W. T. Volkov, E. E. Yakimov, and G. Visimberga, Semiconductors **44**, 1235 (2010).